



# Creep behavior of soft clay subjected to artificial freeze–thaw from multiple-scale perspectives

Jun Li<sup>1,2</sup> · Yiqun Tang<sup>3</sup> · Wei Feng<sup>1,2</sup>

Received: 26 September 2019 / Accepted: 22 April 2020 / Published online: 12 May 2020  
© Springer-Verlag GmbH Germany, part of Springer Nature 2020

## Abstract

Relying on the application of the artificial freezing method on subway tunnel construction, a series of triaxial creep tests were carried out to study the creep behavior changes of Shanghai soft clay subjected to artificial freeze–thaw action. On this basis, MIP tests were conducted with the soil samples before and after creep for comparison to investigate the microstructure changes. The results indicate that freeze–thawed soil produces smaller creep deformation and instantaneous deformation than the unfrozen soil. On a micro-level, during the creep process, the soil skeleton reaches a new structure balance with smaller pore volume and pore area. But the diameter of the maximum pore increases. The change rate of total intrusion volume is a pivotal micro-parameter to evaluate creep strain as there is a good linear relationship between them.

**Keywords** Artificial freezing method · Creep behavior · Microstructure · Soft clay

## 1 Introduction

Artificial ground freezing as an auxiliary ground improvement technique is now widely used in the subway engineering [6, 11, 31]. By freezing selected areas of the ground, artificial ground freezing can provide support for excavations or to cut off water seepage to guarantee the safety of engineering construction and overcome the difficulties [19, 32]. During the frozen process, the soil particles are bonded together by the ice within the soil and the strength of frozen soil increases significantly [10, 14, 19, 21, 40]. And the following thawed process results in the structural rearrangement and changes the structure of the soil particle configuration, which can

influence the deformation characteristics and strength properties of the soil [3, 4, 26, 27, 42, 45]. The long-term deformation and low soil strength can not only affect the normal operation of the subway but also cause damage to the surrounding building [16, 22]. Therefore, it is essential to investigate the freeze–thaw effect on the soil deformation behavior, especially the creep behavior, because the long-term compression has become an important subway engineer issue [29, 30]. The primary purpose of the present paper is to explore the creep behavior response for the freeze–thaw process.

The creep properties which characterize their compression behaviors under long-term constant effective stress are one of the most important engineering deformation properties of soft soil. During the past decades, the researches of soil creep behavior have developed in a variety of directions. And the development of previous work relied on the update of test methods and instruments both for laboratory and field experiments. To be more specific for laboratory tests, till now, the oedometer tests, uniaxial compression tests, triaxial compression tests, and large-scale laboratory experiments are the main test methods concerning the macro-performance. Wu et al. [37] conducted a group of oedometer tests to find the relationship between the creep coefficient and the vertical effective stress. Xu et al. [38] demonstrated the creep performance

✉ Jun Li  
lijun0728@bjfu.edu.cn

Yiqun Tang  
tangyiqun2@mail.tongji.edu.cn

<sup>1</sup> Department of Civil Engineering, Beijing Forestry University, Beijing 100083, People's Republic of China

<sup>2</sup> Key Laboratory of State Forestry Administration on Soil and Water Conservation, Beijing Forestry University, Beijing 100083, People's Republic of China

<sup>3</sup> Department of Geotechnical Engineering, Tongji University, Shanghai 200092, People's Republic of China

of frozen soil by simulating some uniaxial compression tests at different strain rates. Arenson et al. [1], Wang et al. [36] and Zhou et al. [44] tried to explore the creep behavior of soil by controlling various test condition of triaxial compression tests. Harris et al. [7] made a physical modeling of gelifluction and frost creep with a 5 m\*5 m square refrigerated tank. In recent years, the centrifuge experiment began to put into use for soil deformation [8], but its high cost limits the application and promotion. With the deepening of research, the researcher shifted the focus on the micro-level. Tests of mercury intrusion porosimetry (MIP), scanning electron microscopy (SEM) and X-ray CT are conducted to study the intrinsic link between the microscopic characteristics and creep behavior [2, 23, 46]. With the help of these test methods data, the main research of soil creep behavior can be divided into two groups roughly. The first one deals with the soil creep model which is the mathematical description of the time. These models can be roughly divided into the four categories: component model, yield surface model, endochronic model and empirical model [12, 15, 18, 25, 34, 39]. The second aspect is about the creep mechanism considering influence factors such as soil type, soil physical characteristics, mineral content, drainage condition, stress rate, confining pressures, loading history and so on [2, 13, 41, 43]. Among these research objects, frozen soil as one special soil type has received much attention in the past decades. Because of the composition complexity of frozen soil which contains ice and water at the same time, it expresses more complex mechanics characteristics than the unfrozen soil [20]. Comparing the research of frozen soil, study on the thawing stage is relatively less as not only seasonally frozen soil but also artificial frozen soil have endured a freeze–thaw process. Existing researches reach an agreement that freeze–thaw action has a significant influence on the physical and mechanical properties of soil. Viklander [33] proposed a concept of residual void ratio to explain the opposite response of dense and loose soil for freeze–thaw. Simonsen et al. [25, 26], Ma et al. [17] and Zhang et al. [42] poured attention into the deformation behavior during freeze–thaw. Zhou et al. [45] put forward a constitutive model considering the freeze–thaw and confining pressure effect. Furthermore, as all the property change is a reflection of internal structure variation, quite a few of the interpretation on micro-level was presented. Zhang et al. [42] measured the unfrozen water content at various sub-freezing temperatures with nuclear magnetic resonance. Cui et al. [4] and Xu et al. [38] studied on the meso-structural characters after freeze–thaw cycling by the SEM tests. Mercury intrusion porosimetry (MIP) as a quantitative test method is also wildly used in explore the freeze–thaw influence [5, 35]. Therefore, analysis from multiple-scale perspectives may provide a broader research way.

Although many studies of soil creep behavior subjected to freeze–thaw cycle have reported, the basic relationship between the creep property and microstructure has never been satisfactorily explained. So the purpose of this paper is to study on the creep behavior change of soft clay subjected to freeze–thaw both from macro- and micro-perspectives.

Based on the background of the artificial ground freezing technique, a group of triaxial creep tests were carried out to study on the creep behavior change of the saturated soft clay induced by freeze–thaw. From the microscopic aspect, MIP tests were conducted with the soil samples to investigate the microstructure change caused by creep. In this paper, three aspects require further attention. The first aspect deals with the comparison of creep behavior before and after freeze–thaw. The second relates to the microstructure change of thawing soft clay caused by creep deformation. The third aspect focuses on the key micro-parameter which can be used to estimate the creep deformation.

## 2 Materials and methods

### 2.1 Soil samples

#### 2.1.1 Unfrozen soil samples

The undisturbed soil samples which were drilled by using Shelby tube samplers were taken from the Shanghai ④ stratum at the depth of 10–14 m near Jiangpu subway station of Line No. 8, which stratum has high water content, large pore ratio, high compressibility, and low strength [22, 31]. The basic physical properties of the sample soil are listed in Table 1 which shows the average value of samples. The samples were cut into cylinders and the length and diameter of the samples are 80.0 mm and 39.1 mm, respectively, based on the geotechnique test regulations of CNS (China Nation Standard).

#### 2.1.2 Freeze–thawed soil samples

The undisturbed soil samples taken out from the Shelby tube were cut down to a length of 140 mm. In order to guarantee the frost heave and thawing settlement without disturbing, both of the horizontal and vertical displacement are not limited. The freezing process was provided by a DW-40 temperature-controlled cabinet, and the temperatures were set to be  $-10\text{ }^{\circ}\text{C}$ ,  $-20\text{ }^{\circ}\text{C}$ ,  $-30\text{ }^{\circ}\text{C}$ , respectively, according to some practical application of artificial ground freezing [6]. Then the frozen soil was kept in a calorstat ( $25\text{ }^{\circ}\text{C}$ ) for thawing. The process is as follows: First, the unfrozen samples were enclosed with plastic wrap

**Table 1** Physical and mechanical properties of soft clay

Natural water content (%)	Void ratio	Density (g/cm <sup>3</sup> )	Dry density (g/cm <sup>3</sup> )	Specific gravity	Plasticity index	Internal friction angle (°)	Cohesion (kPa)
47.1	1.37	1.70	1.16	2.74	17.9	11.5	10

in order to avoid too much water loss. Second, the samples were put into a DW-40 temperature-controlled cabinet with a stable freezing temperature for 48 h. Third, after completely freezing progress, the frozen samples were put in a calorstat with a stable temperature of 25 °C for 24 h [9]. Finally, the freeze–thawed samples were cut into the cylinders with the same size as those unfrozen soil samples ( $\Phi 39.1 \times 80$  mm).

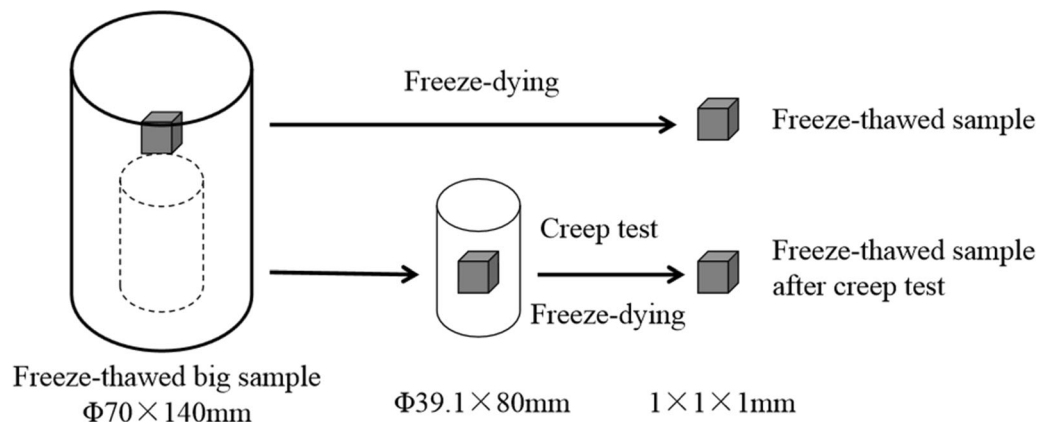
### 2.1.3 Mercury intrusion porosimetry (MIP) test samples

In order to compare the soil microstructure changes caused by freeze–thaw action and creep tests, samples of three stages (unfrozen, thawed and after creep test) have to be reserved. For example, as shown in Fig. 1 from the same freeze–thawed big sample, a  $1 \times 1 \times 1$  mm cube and a cylinder ( $\Phi 39.1 \times 80$  mm) were cut down for MIP and creep test, respectively. Then after the creep test, a  $1 \times 1 \times 1$  mm cube from the middle of the cylinder sample was also achieved to conduct the MIP test. In addition, the freeze-drying technique which can maintain the original pore structure was used to dehydrate the saturated soil samples for MIP tests. The microstructure before and after creep tests can be compared by the two cube samples.

## 2.2 Testing apparatus and methodology

### 2.2.1 Creep tests

The TSS10 triaxial creep test system produced by Changchun experiment research institution was utilized for the text. This creep test system can apply a stable axial load and radial load at the same time and measure the displacement and pore pressure during the tests. The basic control parameters are determined as follows: (1) Cell pressure: in consideration of the depth of soil samples, the back pressure was set to be 100 kPa while the effective radial pressures were 70 kPa, 105 kPa, and 140 kPa, respectively. (2) Deviator pressure: due to the limitation of creep test time, the load mode was chosen to be the step load method as the load increment was constant of each step. Based on the result of triaxial shear texts, the shear strength of unfrozen soil with the effective cell pressure 70 kPa is  $q_f = 74$  kPa. If the total step number is  $n = 6$ , the load increment  $q_f/n = 74/6$  kPa = 12.3 kPa. Therefore, the deviator pressure of six steps can set to be 15.0 kPa, 30.0 kPa, 45.0 kPa, 60.0 kPa, 75.0 kPa, 90.0 kPa, respectively. Because with higher effective cell pressure, the shear strength will be larger than 74 kPa, the six deviator pressures are also available for creep tests with 105 kPa and 140 kPa cell pressure. All of the relative test control parameters are summarized in Table 2.

**Fig. 1** Freeze–thawed sample preparation process

**Table 2** Control parameters of creep tests

Effective cell pressure (kPa)	Freezing temperature (°C)	Deviator pressure (kPa)					
70	Unfrozen	15	30	45	60	75	90
	– 10	15	30	45	60	75	90
	– 20	15	30	45	60	75	90
	– 30	15	30	45	60	75	90
105	– 10	15	30	45	60	75	90
140	– 10	15	30	45	60	75	90

### 2.2.2 Mercury intrusion porosimetry (MIP)

In order to investigate the microstructure changes caused by creep, the soil samples before and after creep tests were reserved to conduct MIP tests for comparison. On the purpose of guaranteeing the reliability of MIP test results, each group of soil samples before and after creep were acquired from the same soil sample. So the result can express the accurate change of microstructure caused by creep. The results of unfrozen soil and thawing soil with  $-10\text{ }^{\circ}\text{C}$  were discussed as follows. Mercury intrusion porosimetry (MIP) is a mature method for microstructure study which can provide the basic information of the porous characteristics of soils: porosity, pore volume, pore size distribution, and density. It is important to realize that MIP is limited to measuring the diameter of the neck of the pores, whereas the diameter of the pores may vary with length throughout the channel. From the pressure-intrusion data, the pore volume and its distribution were determined. Mercury intrusion porosimetry involves the measurement of the volume of mercury injected into the porous medium with increasing applied pressure [24]. And it is based on the premise that a nonwetting liquid (one having a contact angle greater than  $90^{\circ}$ ) will only intrude capillaries under pressure. The calculate relationship between the pressure and capillary diameter is described by Washburn (Eqs. 2 and 3). The MIP technique is widely used because of its ease and simplicity. However, it does not measure the true distribution of sizes for pore geometries found in cement-based materials. For these systems, large internal pores are accessible by very narrow throats. The MIP technique misrepresents the size of these pores as having the diameter of their throats. This bias is referred to as the “ink bottle” effect [35].

$$P\pi r^2 L = T_s \cdot 2\pi r / \cos \theta \quad (2)$$

$$P = \frac{2T_s \cos \theta}{r} \quad (3)$$

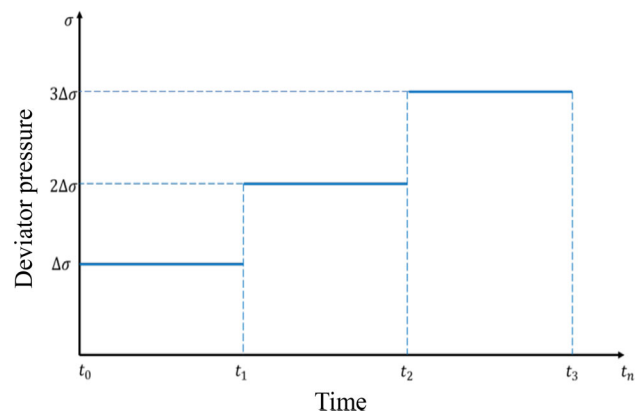
where  $P$  is the required pressure;  $L$  is the length of the pore;  $r$  is the smallest diameter of an opening into which mercury will penetrate at pressure  $P$ ;  $T_s$  is the surface tension

coefficient of mercury and  $T_s = 0.473\text{--}0.485\text{ N/m}$ ;  $\theta$  is the contact angle of import liquid and solid material while  $\theta = 117^{\circ}\text{--}141^{\circ}$ .

As for this study, Mercury porosimetry experiments were performed using a Micromeritics Autopore IV 9500. In order to keep the original structure of soil samples at the extreme, the -drying method which can maintain the original pore structure was used to remove moisture from the porous structure before the MIP tests. Besides some scanning electron microscopy (SEM) were conducted as an assistant method for qualitative analysis.

## 3 Results and discussion

For purpose of more specific data analysis, the test data of soil displacement generated by step loading have been transformed into data caused by one stable loading with the Chen Applying Method which is proposed by Tan Tjiong kie [28]. The typical step loading of creep tests is shown in Fig. 2 and the process of creep data transformation is shown in Fig. 3. Within the time range of  $t_0$  to  $t_1$ , creep deformation generates because of first step loading  $\Delta\sigma$ . If the axial load keeps stable, that is there is no more step loading applying on the soil sample, the creep deformation will increase along with the dotted curve in Fig. 3.

**Fig. 2** Typical step loading of creep text

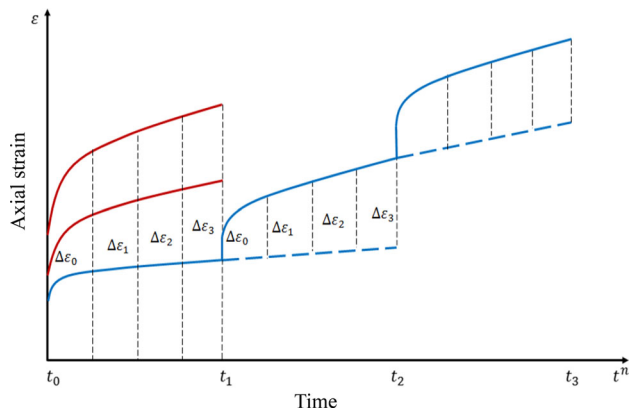


**Fig. 3** Creep data transformation of Chen Applying Method

Therefore, the loading increment of the second step induces the deformation which is equal to the difference value between the solid curve and the dotted curve. The creep curve of stable loading  $2\Delta\sigma$  can be acquired by the curve of two steps loading ( $\Delta\sigma$  and  $2\Delta\sigma$ ). And by this analogy, six creep curves of six different stable loading (15.0 kPa, 30.0 kPa, 45.0 kPa, 60.0 kPa, 75.0 kPa, 90.0 kPa) can be gotten only by one curve of six-step loading.

### 3.1 Full rheological curves

The full rheological curves of unfrozen soil and freeze-thawed soil with three different freezing temperatures are shown in Fig. 4. Except for the unfrozen soil sample under 90 kPa deviator stress fails, at last, the creep deformation of the unfrozen soil and freeze-thawed soil tend to be stable. A similar change rule is suitable for both unfrozen soil and freeze-thawed soil. Distinctly, all the axial strain curves can be divided into two stages—rapidly increasing stage and damply increasing stage. In the first stage, the axial strain increases rapidly and most axial strain accumulates in this stage. Then, in the second stage, the incremental rate of strain gradually reduces and has a tendency to decay to zero.

Comparing the axial strain of unfrozen soil and freeze-thawed soil, it is obvious that unfrozen soil produces more deformation than all the three kinds of freeze-thawed soil under the same loading condition. Further, the axial strain range of unfrozen soil is about 1.2–22% while the ranges of freeze-thawed soil are 0.8–8%, 0.6–10%, 1–9% corresponding with  $-10\text{ }^{\circ}\text{C}$ ,  $-20\text{ }^{\circ}\text{C}$ ,  $-30\text{ }^{\circ}\text{C}$ , respectively. There is no much difference between the creep strain of freeze-thawed soil with three different freezing temperatures. Therefore, the freeze-thaw process has a great influence on the creep behavior of soft clay, but apparent correlation does not exist between the axial strain and the freezing temperature. No matter for unfrozen soil and freeze-thawed soil, an instantaneous deformation occurs at

the moment of applying axial load. And the instantaneous deformation increases with the growth of deviator loading. With the same loading condition, the unfrozen soil occupies larger instantaneous deformation than the freeze-thawed soil which has better deformation resistance ability. Undergoing the freeze-thaw process, the water in soil transforms from water to ice and back to water. The frost heave can lead to expanding of soil pore, and thaw collapse makes rearrange of soil structure. Apparently, after the freeze-thaw action, the deformation property degrades. In conclusion, caused by the freeze-thaw process, the three kinds of freeze-thawed soil produce smaller creep deformation and instantaneous deformation than the unfrozen soil under the same loading condition. But the value of freezing temperatures has a slight influence on the creep deformation.

### 3.2 Strain rate–time double logarithmic curves

A study on the relationship between strain rate and time is significant for research on creep behavior of soil. Figure 5 shows the strain rate–time double logarithmic curves of unfrozen soil and freeze-thawed soil. Some conclusions can be obtained as follows. Firstly, the logarithmic curves of strain rate and time express approximate linearity and the strain rate decreases with the increase in time and close to zero at last; secondly, both for the unfrozen soil and freeze-thawed soil, the curves almost keep parallel to each other, and the strain rate with larger deviator stress is larger than that with smaller deviator stress. The strain rate needs less time to decrease to zero with smaller deviator stress. Lastly, under the same test condition, the strain rate of freeze-thawed soil is smaller than that of unfrozen soil. The freeze-thaw process can not only reduce the creep deformation of soft clay but also decrease the strain rate. The strain rate–time double logarithmic curves of freeze-thawed soil with different freezing temperatures are quite similar, so the change of strain rate corresponding to the value of freezing temperature has no apparent rule.

### 3.3 Microstructure changes

Two kinds of microstructure changes caused by freeze-thaw and creep are present in the following part. Before the quantitative analysis, Fig. 6 demonstrates the visible change of pores and particles with the amplification factor of 2000. The particle aggregation pattern of unfrozen soil is mainly side–side and side–surface connection. Due to the freezing process, the ice invades and enlarges the pores, so the cementation body between soil particles is damaged causing disintegration and dispersion of the soil particles to some extent [4]. Then during the following thawing period, the original structure collapses with a great deal of pore

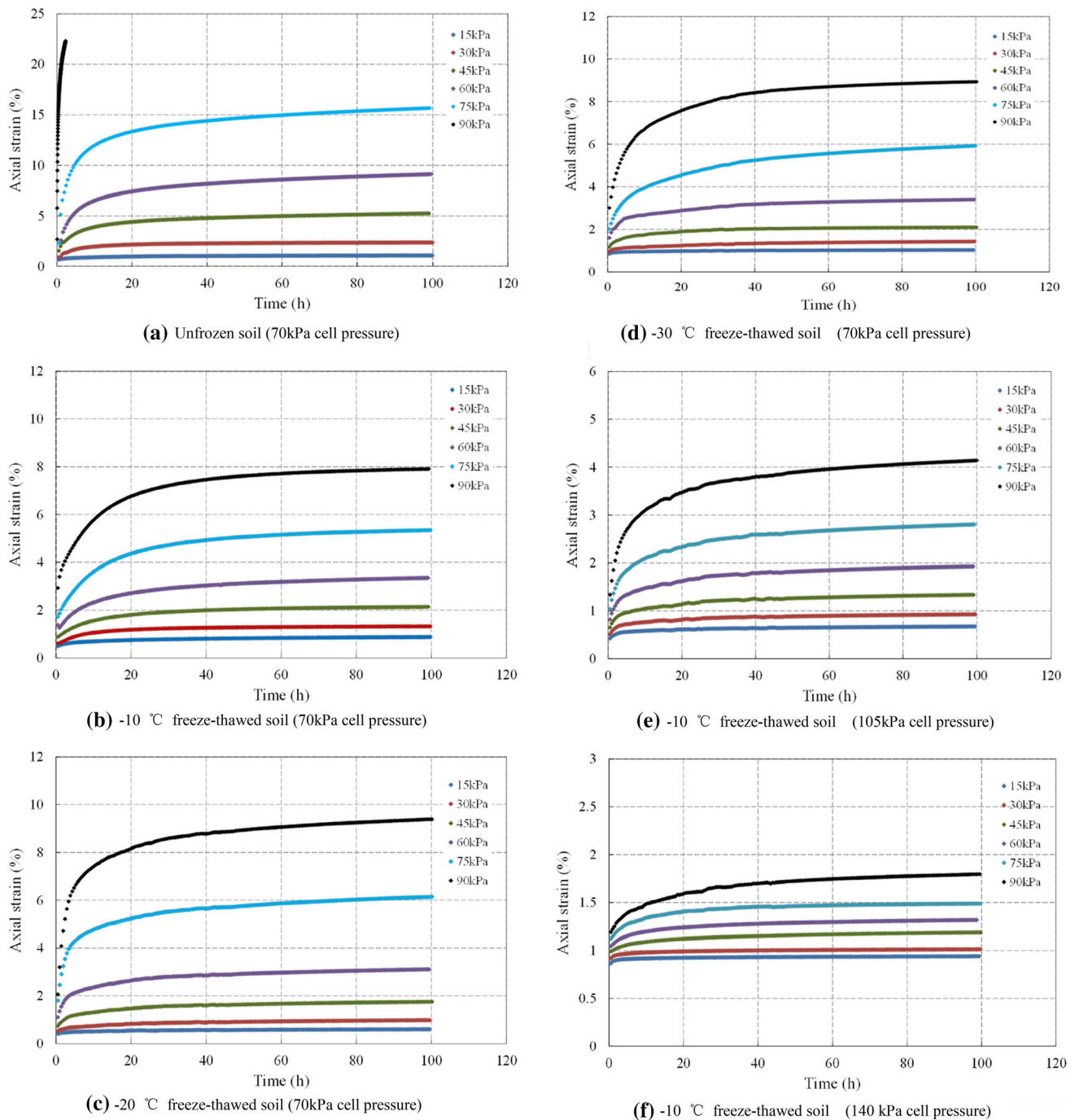


**Fig. 4** Full rheological curves

squeezing together leading to the reduction in the equivalent pore diameters. Furthermore, the pores keep on compressing with particles converge together during the creep tests. As a result, the distributions of pore orientation angles tend to be more directional as shown in Fig. 6. More detailed microstructure changes are detected by the MIP tests as follows.

### 3.3.1 Changes of microstructure caused by freeze-thaw action

The relationship between the accumulated mercury volume and intrusion pressure of undisturbed soil and freeze-thawed soil with different freezing temperatures is shown in Fig. 7. The cumulative mercury volume of unfrozen soil is about 0.26 mL/g, which is larger than that of freeze-thawed soil. As a consequence, one aspect of

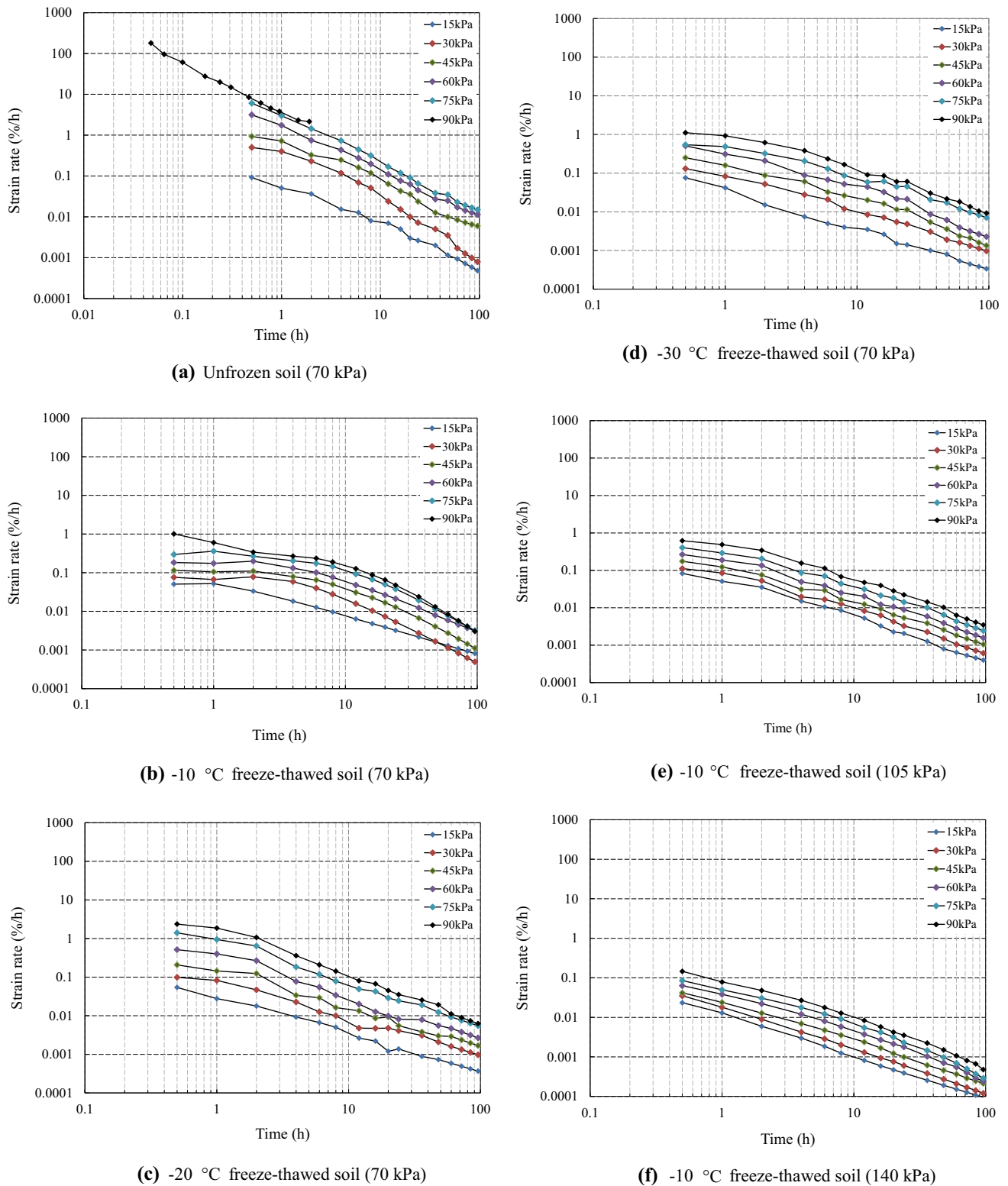


**Fig. 5** Strain rate–time double logarithmic curve

microstructure change performs as the reduction in the total pore volume. Compared the results of freeze–thawed soil, the – 30 °C freeze–thawed soil occupies the largest total

pore volume (0.23 mL/g), following by the – 10 °C freeze–thawed soil (0.22 mL/g) and the – 20 °C freeze–thawed soil (0.21 mL/g). The range of the threshold value

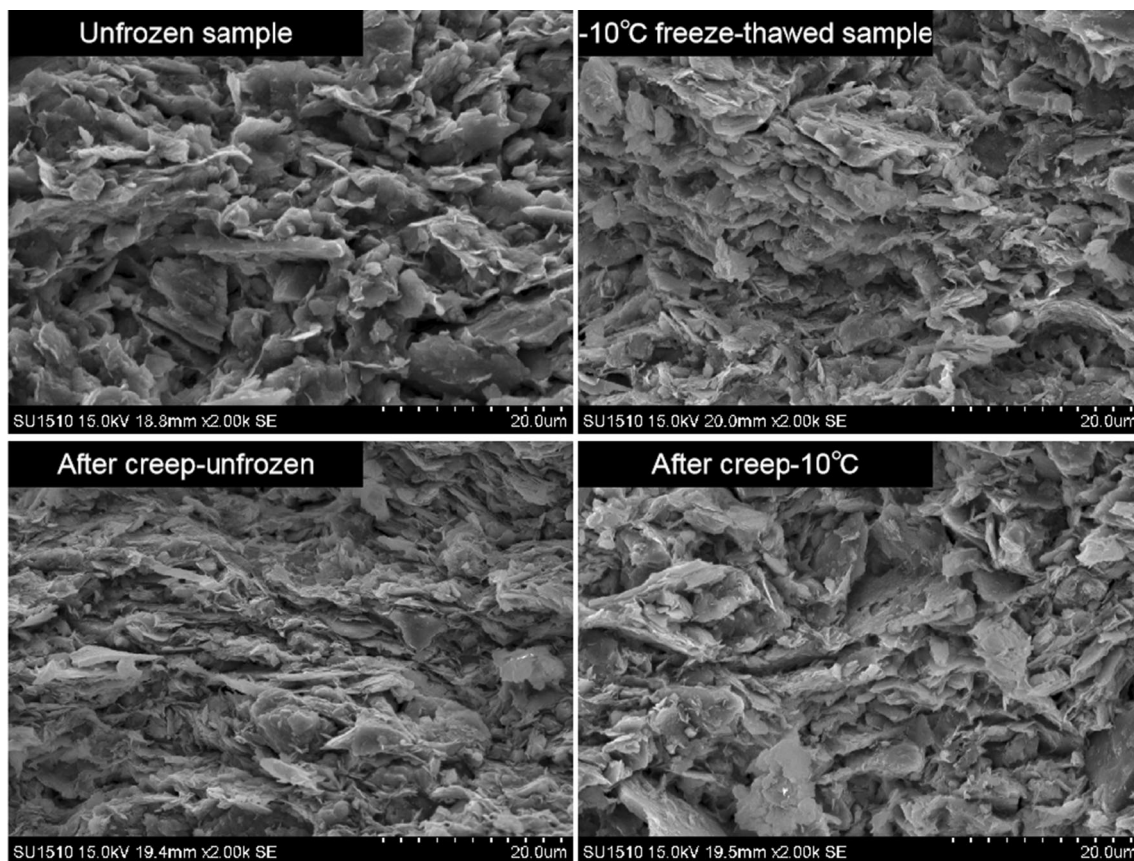


Fig. 6 SEM images of different stages

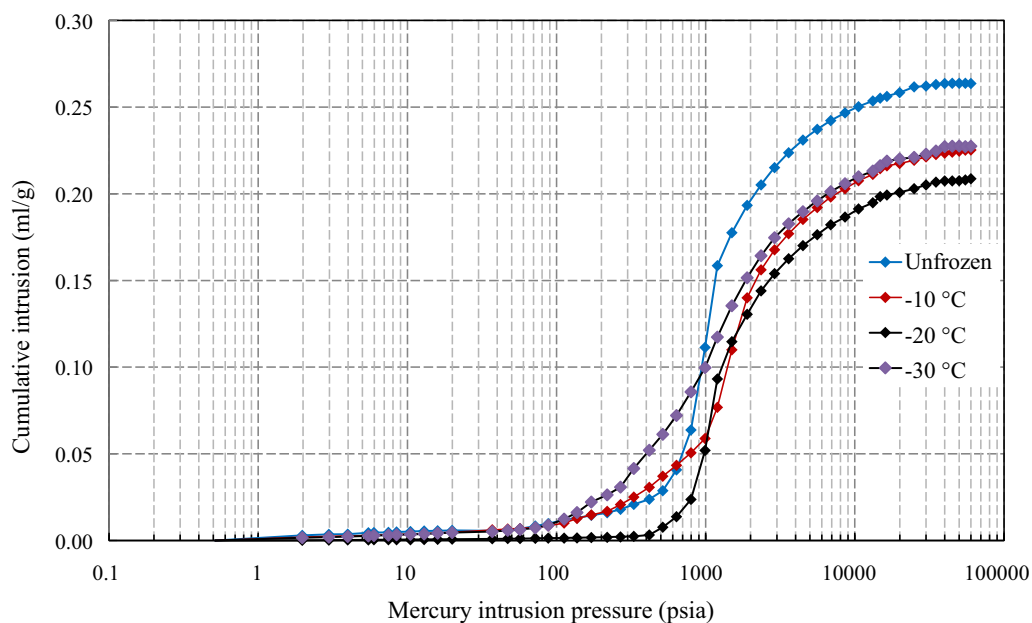


Fig. 7 Cumulative intrusion volume vs intrusion pressure curve with different freezing temperatures

of intrusion pressure for undisturbed soil and freeze-thawed soil is approximately 100 psia to 1000 psia and  $-20\text{ }^{\circ}\text{C}$  freeze-thawed soil has the maximum threshold

value of intrusion pressure which is about 950 psia. Therefore, the freeze-thaw process decreases the soil pore volume, while there is less space to generate compressional



deformation. That's why freeze–thawed soil has smaller creep deformation as shown in Fig. 4.

Figure 8 gives information about the relationship between the accumulated pore area and pore size diameter with different freezing temperatures. The freeze–thaw process induces a reduction in total pore area, which has the same influence on the total pore volume of soft clay. As for the freeze–thawed soil, the total pore area of soil with  $-10\text{ }^{\circ}\text{C}$  freezing temperature is the largest, following by soil with  $-20\text{ }^{\circ}\text{C}$  and  $-30\text{ }^{\circ}\text{C}$  freezing temperatures. Therefore, the extent of freeze–thaw influencing on the pore area increases with the decrease in freezing temperatures.

The pore size distribution is demonstrated in Fig. 9, and the distribution is similar to normal distribution. No matter for the undisturbed soil and freeze–thawed soil, the most probable pore sizes are restricted in the range of 100–200 nm. However, the proportion of the most probable pore size for the undisturbed soil is larger than that of freeze–thawed soil. That is to say, compared with freeze–thawed soil, the pore size distribution of undisturbed soil is relatively concentrated. For the following reasons, during freezing, the water within pores is frozen into ice, so the soil pores are filled with ice which has a larger volume than water. The connection of particles suffers damage leading to the disintegration and dispersion of the particles. In the next thawing stage, ice melts into water, and the shrink of soil pores gives rise to the collapse of soil skeleton, because the cementation body between particles has already been weakening. In the process of rebalancing,

some large pores close or shrink while some smaller pores gather together and the pore size distribution is relatively less concentrated compared with unfrozen soil. In conclusion, the freeze–thaw process results in the rearrangement of soil microstructure by enlarging the range of pore size and making it much more mean.

### 3.3.2 Changes of microstructure caused by creep

During the creep process, because of the compression of soil caused by stable deviator loading, the microstructure of soft clay is experiencing rearrangement to establish a new structure balance. By comparing the micro-characteristics parameters before and after creep, the mechanism of creep deformation can be discussed on a micro-level. Figures 10, 11 and 12 demonstrate the change of accumulated mercury volume (pore volume), pore area and pore size distribution of unfrozen soil separately. The microstructure changes can be summarized as follows: (1) Based on the mercury intrusion curves (Fig. 10), it is clear that the total pore volume decreases to a great degree after creep, and this phenomenon is caused by the pore closure induced by soil compression. (2) Comparing the mercury extrusion curves (Fig. 10) before and after creep, the volumes of residual mercury are almost the same, so the efficiency of mercury withdrawal of soft clay falls down after creep. (3) Creep has a significant influence on the pore area as the accumulated pore area has an obvious decrease trend after creep (Fig. 11). (4) The pore size distribution of soft clay tends to be more mean after creep because of the enlargement of

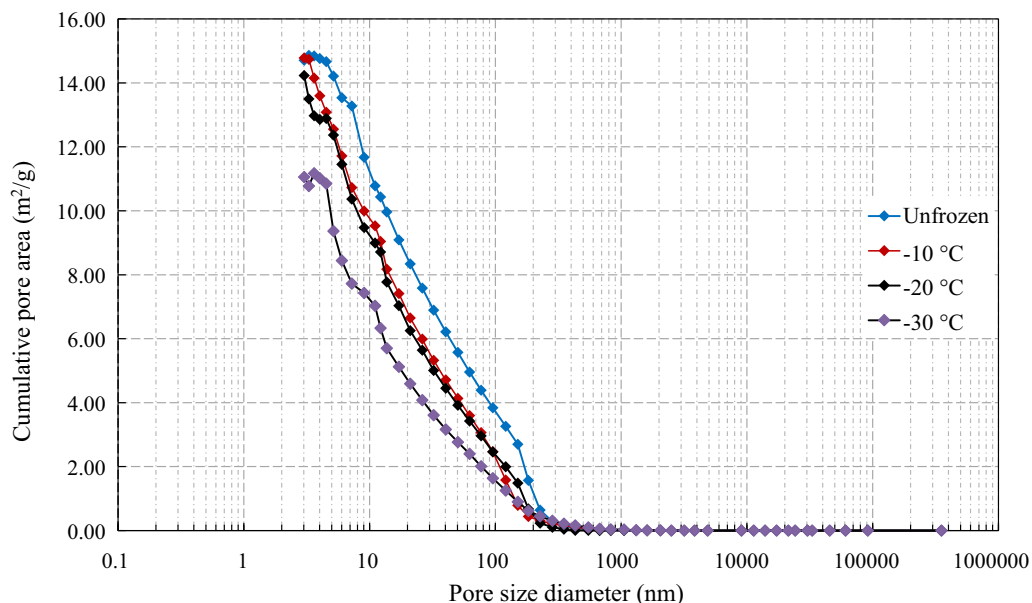


**Fig. 8** Cumulative pore area vs intrusion pressure curve with different freezing temperatures

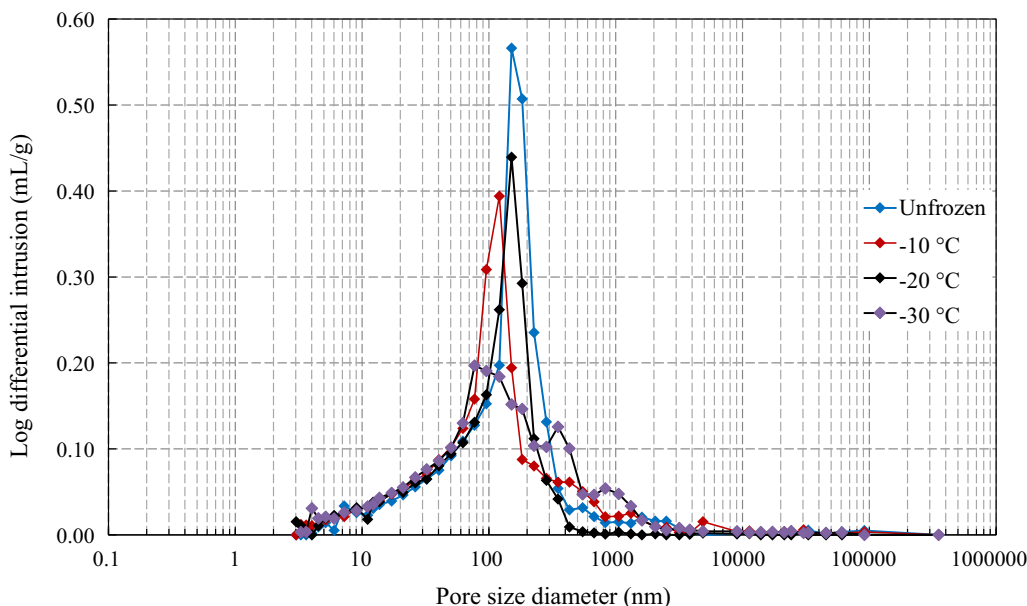


Fig. 9 Pore size distribution with different freezing temperatures

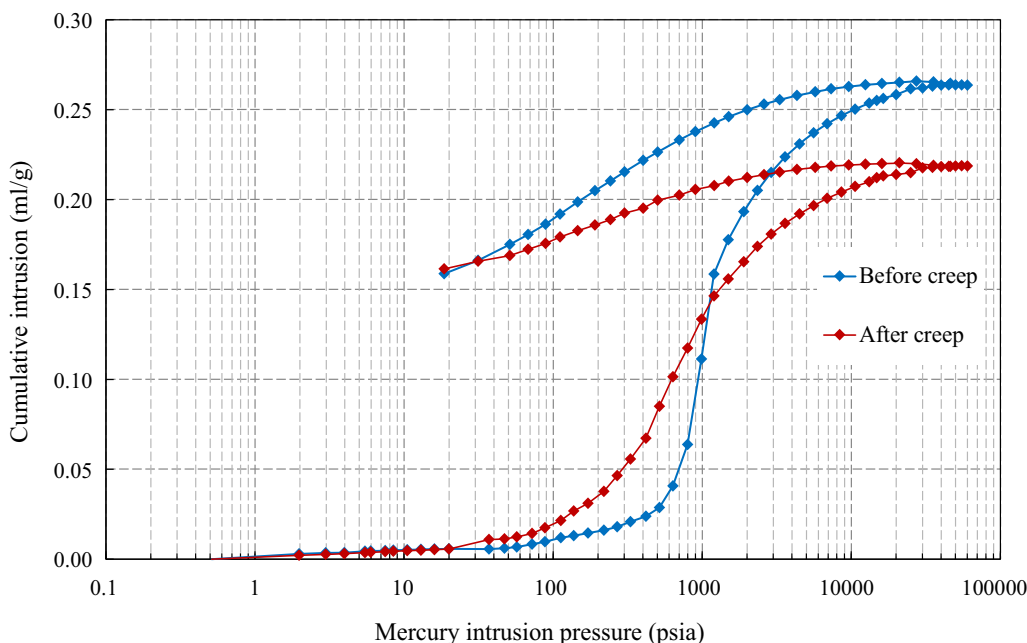
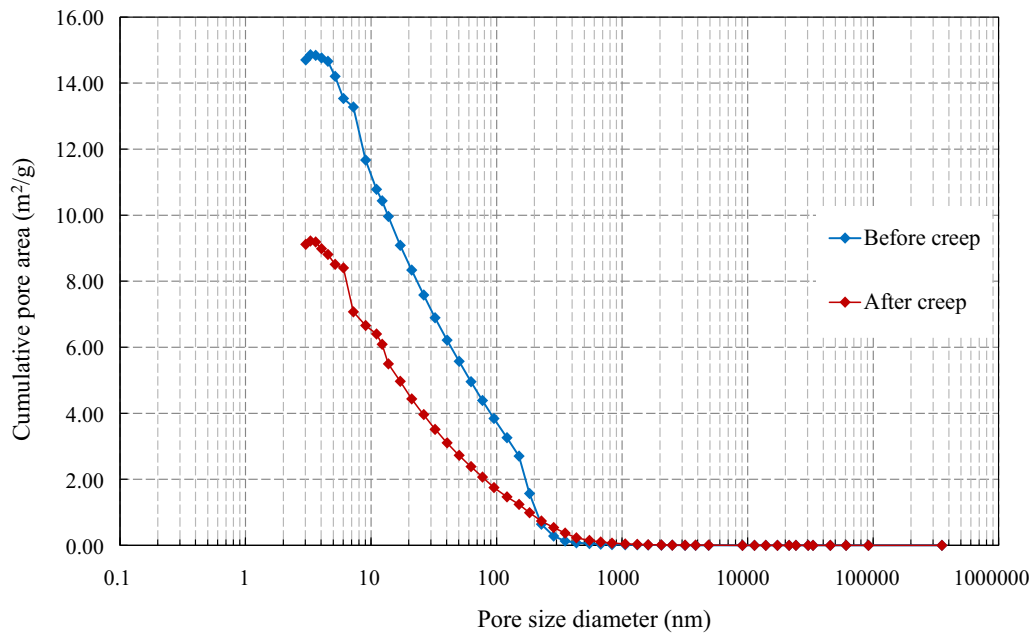


Fig. 10 Cumulative intrusion volume vs intrusion pressure curve of unfrozen soil

pore size range and reduction in proportion corresponding with the most probable pore size (Fig. 12). (5) As the most probable pore size of soil after creep increases from 151 nm to 284 nm, the amount of larger pore raises at the same time.

Taking the  $-10\text{ }^{\circ}\text{C}$  freeze-thawed soil with three cell pressures (70 kPa, 105 kPa, 140 kPa) for example, the microstructure changes resulting from creep text of freeze-

thawed soil are discussed in Figs. 13, 14 and 15, respectively. Similar change rules are showing by comparison with the unfrozen soil. The microstructure changes can be summarized as follows: (1) The total pore volume decreases after creep resulting from the pore closure induced by soil compression, but the decreasing extent is smaller than that of the unfrozen soil (Fig. 13). (2) Comparing the mercury extrusion curves (Fig. 13) before and



**Fig. 11** Cumulative pore area vs pore size diameter curve of unfrozen soil

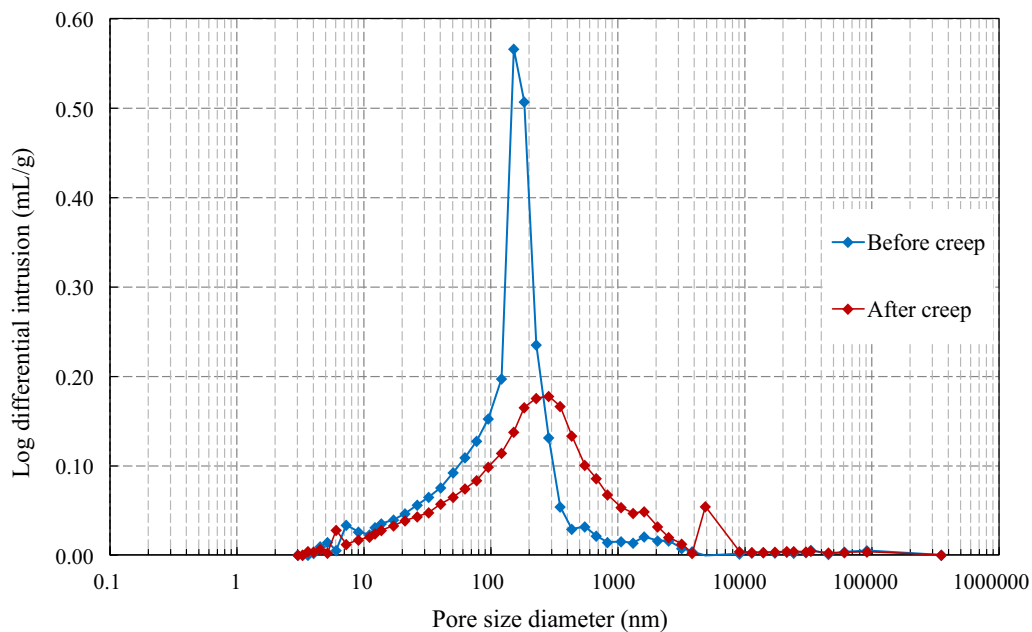


**Fig. 12** Pore size distribution of unfrozen soil

after creep, the volumes of residual mercury are almost the same. (3) Creep has a significant influence on the pore area as the accumulated pore area has an obvious decrease trend after creep (Fig. 14). (4) The pore size distribution of freeze–thawed soil tends to be more mean after creep shown as Fig. 15. The most probable pore size of freeze–thawed soil increases from about 100 to about 260 nm after creep.

In conclusion, along with the creep deformation, the soil skeleton suffers from compression, so some large pores vanish or close. According to the pore size distribution result, the diameter of maximum pore increases, that is because some small pores gather producing large pores. So the amount of larger pore increases. At last, the skeleton reaches a new structure balance with smaller pore volume and pore area.

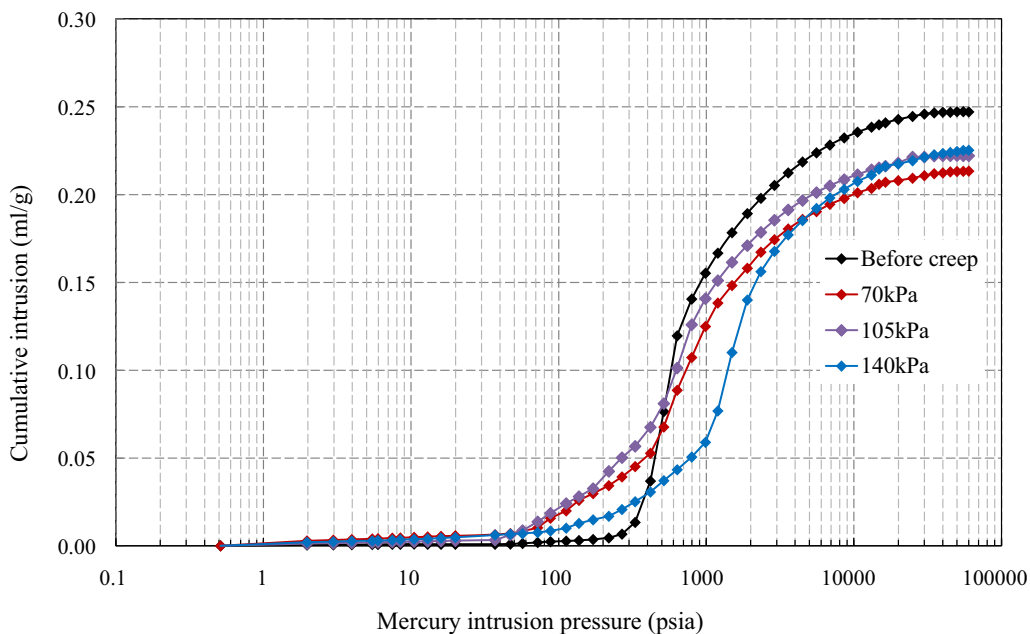


Fig. 13 Cumulative mercury volume vs intrusion pressure curve of  $-10\text{ }^{\circ}\text{C}$  freeze-thawed soil

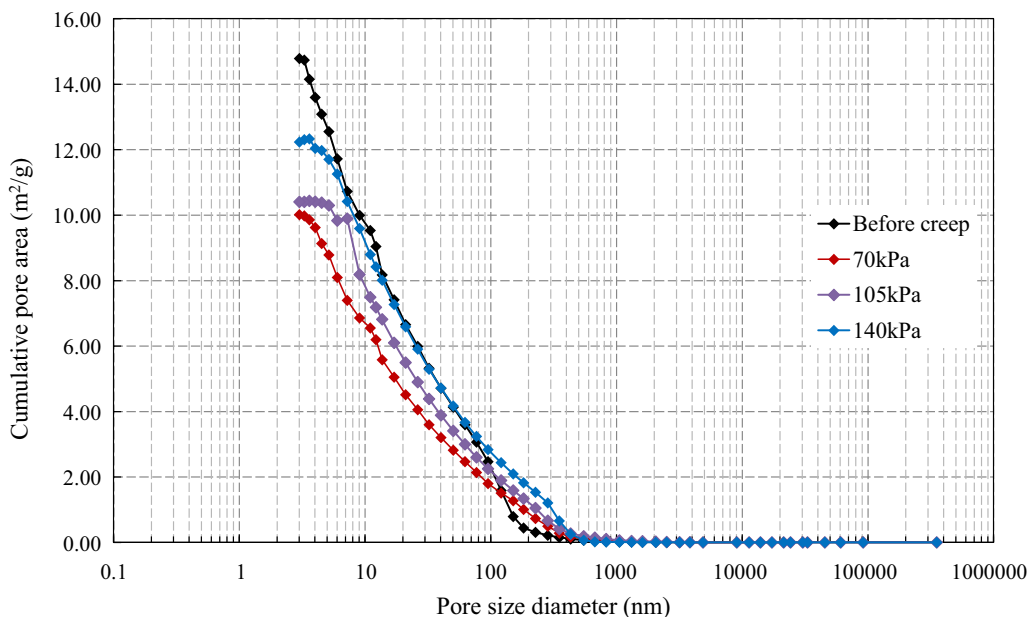


Fig. 14 Cumulative pore area vs pore size diameter curve of  $-10\text{ }^{\circ}\text{C}$  freeze-thawed soil

### 4 Creep strain and micro-characteristics

The creep deformation can lead to the rearrangement of microstructure. In order to investigate the relationship between them and find a superior parameter to indicate deformation, two typical micro-characteristics (total pore area, total intrusion volume) were chosen. The difference

value of the micro-characteristics parameters was calculated to establish a relationship with the creep deformation.

#### 4.1 Total pore area

The total pore area of soil samples before and after creep tests is shown in Fig. 16, and it is clear that the creep results in reduction in total pore area. As the change rate

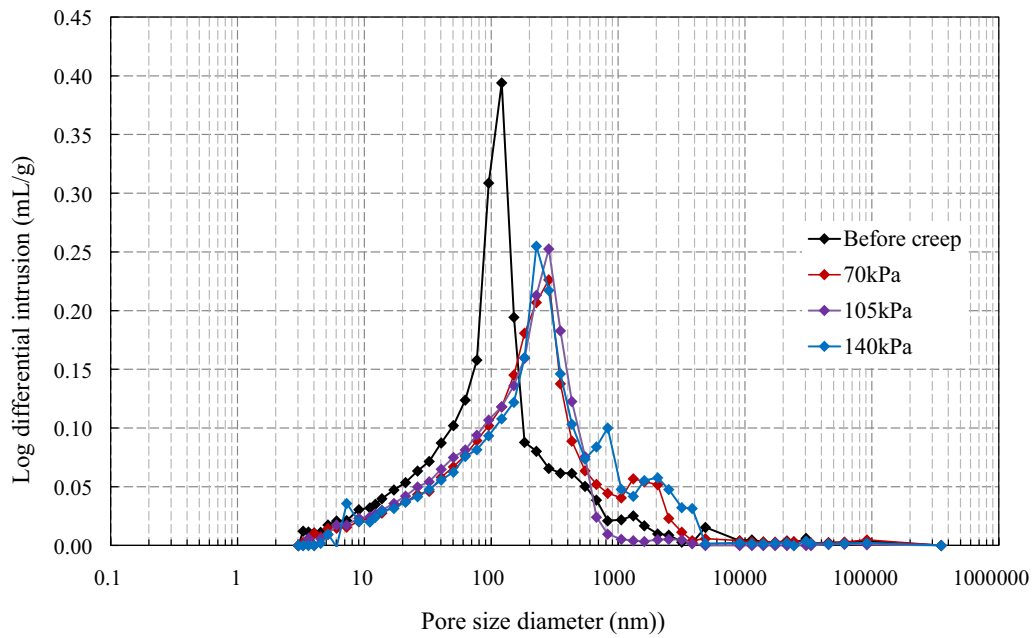


Fig. 15 Pore size distribution of - 10 °C freeze-thawed soil

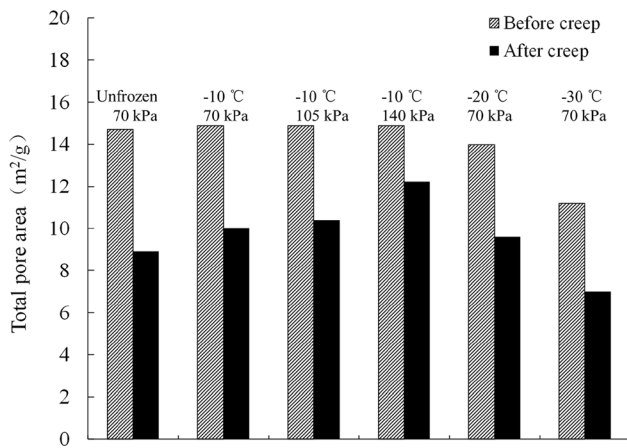


Fig. 16 Change of total pore area caused by creep strain

conducts well to demonstrate the variation degree of characteristic parameters, it is chosen to build relation with the creep strain. Therefore, the change rate of the total pore

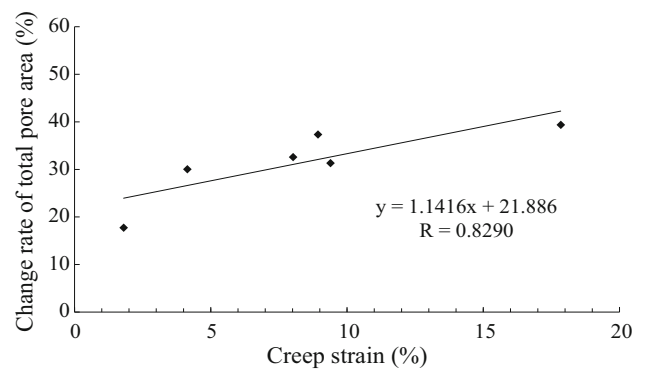
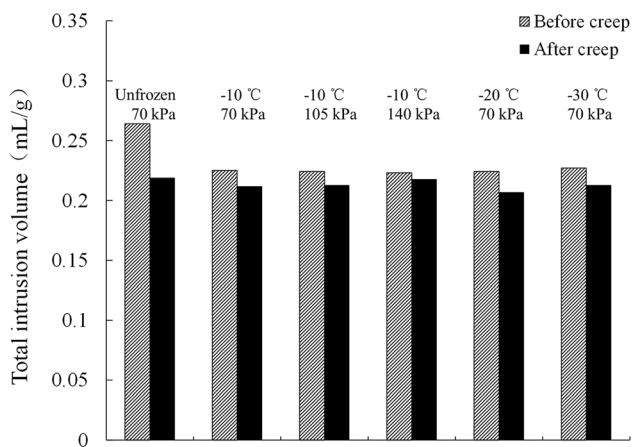


Fig. 17 Relationship between change rate of total pore area and creep strain

area and creep strain is summarized in Table 3. The relationship between the change rate of total pore area and creep strain is established (shown in Fig. 17). The following conclusions can be drawn from the study.

Table 3 Statistical results for total pore area caused by creep strain

Freezing temperature (°C)	Creep test cell pressure (kPa)	Creep strain (%)	Total pore area (m <sup>2</sup> /g)			
			Before creep	After creep	Difference value	Change rate (%)
Unfrozen	70	17.84	14.70	8.91	5.79	39.390
- 10	70	8.02	14.87	10.02	4.85	32.619
- 10	105	4.14	14.86	10.39	4.47	30.069
- 10	140	1.80	14.87	12.23	2.64	17.759
- 20	70	9.39	13.98	9.60	4.38	31.339
- 30	70	8.93	11.19	7.01	4.18	37.359



**Fig. 18** Change of total intrusion volume caused by creep strain

1. For unfrozen soil and thawing soil, the creep can lead to a decrease in the total pore area.
2. The change rate of unfrozen soil is larger than that of thawing soil.

3. For the thawing soil with the same freezing temperature, the change rate is larger with lower cell pressure.
4. Although the change rate increases with the creep strain, there is no obvious linear relationship as the correlation coefficient  $R$  is only 0.8290.

### 4.2 Total intrusion volume

From Fig. 18, it is clear that the creep also causes a decrease in the total intrusion volume. The change rate of total intrusion volume and creep strain is displayed in Table 4. To be more specific, Fig. 19 indicates a good linear relationship between the change rate of total intrusion volume and creep strain with  $R = 0.9706$ . Taken together with the previous study on the total pore area, the value of creep strain and the change rate of total intrusion volume have a clearer linear relation. On a micro-level, the total intrusion volume is a superior choice to indicate the creep deformation.

**Table 4** Statistical results for total intrusion volume caused by creep strain

Freezing temperature (°C)	Creep test cell pressure (kPa)	Creep strain (%)	Total intrusion volume (mL/g)			
			Before creep	After creep	Difference value	Change rate (%)
Unfrozen	70	17.84	0.264	0.219	0.045	17.045
- 10	70	8.02	0.225	0.212	0.013	5.778
- 10	105	4.14	0.224	0.213	0.011	4.911
- 10	140	1.80	0.223	0.218	0.005	2.242
- 20	70	9.39	0.224	0.207	0.017	7.589
- 30	70	8.93	0.227	0.213	0.015	6.608

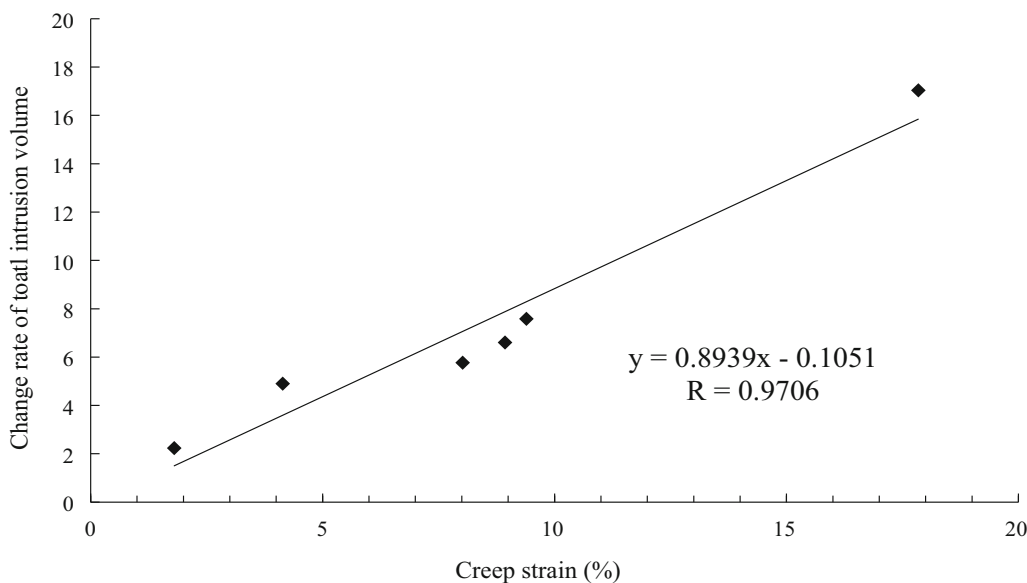


**Fig. 19** Relationship between change rate of total intrusion volume and creep strain

## 5 Conclusions

Based on the artificial freezing method, this study characterizes the creep behavior of freeze–thaw soft soil with creep triaxial tests and Mercury intrusion porosimetry. Meaningful conclusions are summarized as follows:

1. Freeze–thawed soil produces smaller creep deformation and instantaneous deformation than the unfrozen soil under the same loading condition. But the value of freezing temperatures has a slight influence on the creep deformation.
2. The freeze–thaw process induces the decrease in pore volume and pore area, resulting in the rearrangement of soil microstructure by enlarging the range of pore size and making it much more mean.
3. During the creep process, the soil skeleton reaches a new structure balance with smaller pore volume and pore area. The diameter of maximum pore increases, because some small pores gather producing large pores and the amount of larger pores increase.
4. The value of creep strain and the change rate of total intrusion volume have a linear relationship. The pore volume is a key parameter to indicate creep deformation.

**Acknowledgements** The investigation was supported by the Fundamental Research Funds for the Central Universities of China (No. BLX201618) and the National Natural Science Foundation of China (Grant Nos. 31800610 and 41072204). The authors are deeply indebted to the financial supporters. And we gratefully acknowledge the Beijing Municipal Education Commission for their financial support through Innovative Transdisciplinary Program “Ecological Restoration Engineering”.

## References

1. Arenson LU, Springman SM (2005) Triaxial constant stress and constant strain rate test on ice-rich permafrost samples. *Can Geotech J* 42(2):412–430
2. Bésuelle P, Viggiani G, Desrues J, Coll C, Charrier P (2014) A laboratory experimental study of the hydromechanical behavior of Boom clay. *Rock Mech Rock Eng* 47:143–155
3. Chamberlain EJ, Gow AJ (1979) Effect of freezing and thawing on the permeability and structure of soils. *Eng Geol* 13(4):73–92
4. Cui ZD, He PP, Yang WH (2014) Mechanical properties of a silty clay subjected to freezing–thawing. *Cold Reg Sci Technol* 98:26–34
5. Dalla Santa G, Cola S, Secco M, Tateo F, Sassi R, Galgaro A (2019) Multiscale analysis of freeze–thaw effects induced by ground heat exchangers on permeability of silty clays. *Geotechnique* 69(2):95–105
6. Fang JH, Zhang ZH, Zhang JY (2009) Application of artificial freezing to recovering a collapsed tunnel in Shanghai metro No. 4 line. *Chin Civ Eng J* 42(8):124–128
7. Harris C, Gallop M, Coutard JP (1993) Physical modeling of gelifluction and frost creep: some results of a large-scale laboratory experiment. *Earth Surf Proc Land* 18(5):383–398
8. Harris C, Davies MCR, Rea BR (2010) Gelifluction: viscous flow or plastic creep? *Earth Surf Proc Land* 28(12):1289–1301
9. He LH (2009) Experimental study on electrical resistivity characteristic of silty clay under uniaxial compression and frozen–thaw cycles. Graduate School of Chinese Academy of Science, Wuhan
10. Hivon E, Sego D (1995) Strength of frozen saline soils. *Can Geotech J* 32(2):336–354
11. Jun H, Liu Y, Li YP, Yao K (2018) Artificial ground freezing in tunnelling through aquifer soil layers: a case study in Nanjing Metro Line 2. *KSCE J Civ Eng* 22(10):4136–4142
12. Leoni M, Karstunen M, Vermeer PA (2008) Anisotropic creep model for soft soils. *Geotechnique* 58(3):215–226
13. Lei HY, Hb Lu, Wang XC, Ren Q, Li B (2015) Changes in soil micro-structure for natural soft clay under accelerated creep condition. *Mar Georesour Geotech* 34(4):365–375
14. Li HP, Zhu YL, Zhang JB, Lin CN (2004) Effects of temperature, strain rate and dry density on compressive strength of saturated frozen clay. *Cold Reg Sci Technol* 39:39–45
15. Liao M, Lai Y, Liu E, Wan X (2016) A fractional order creep constitutive model of warm frozen silt. *Acta Geotech* 12(2):1–13
16. Lin YG, Liao SM, Liu GB (2000) Discussion of influence factors on axial deformation of subway tunnel. *Undergr Space* 20(4):264–267 (in Chinese)
17. Ma L, Qi J, Yu F, Yao X (2016) Experimental study on variability in mechanical properties of a frozen sand as determined in triaxial compression tests. *Acta Geotech* 11(1):61–70
18. Mesri G, Febrescordero E, Shields DR, Castro A (1981) Shear stress–strain–time behavior of clays. *Géotechnique* 32(4):407–411
19. Pimentel E, Sres A, Anagenostou G (2012) Laboratory tests on artificial ground freezing under seepage–flow conditions. *Geotechnique* 62(3):227–241
20. Qi J, Vermeer PA, Cheng G (2006) A review of the influence of freeze–thaw cycles on soil geotechnical properties. *Permafrost Periglac* 17(3):245–252
21. Razbegin VN, Vyalov SS, Maksimyak RV (1996) Mechanical properties of frozen soils. *Soil Mech Found Eng* 33(2):35–45
22. Ren X, Tang Y, Li J, Yang Q (2012) A prediction method using grey model for cumulative plastic deformation under cyclic loads. *Nat Hazards* 64(1):441–457
23. Shi B, Wang BJ, Ning WW (1997) Micromechanical model on creep of anisotropic clay. *Chinese J Geotech Eng* 19(3):7–13 (in Chinese)
24. Sills ID, Aylmore LAG, Quirk JP (1973) A comparison between mercury injection and nitrogen sorption as methods of determining pore size distributions. *Soil Sci Soc Am J* 37(4):535–537
25. Singh A, Mitchell J (1968) General stress–strain–time function for soils. *J Soil Mech Found* 94(1):21–46
26. Simonsen E, Isacsson U (2001) Soil behavior during freezing and thawing using variable and constant. *Can Geotech J* 38(4):863–875
27. Simonsen E, Janoo VC, Isacsson U (2002) Resilient properties of unbound road materials during seasonal frost conditions. *J Cold Reg Eng* 16(1):28–50
28. Tan Tk, Kang WF (1991) On the locked in stress, creep and dilatation of rocks, and the constitutive equations. *Chin J Rock Mech Eng* 10(4):299–312 (in Chinese)
29. Tang YQ, Li J, Wan P, Yang P (2014) Resilient and plastic strain behavior of freezing–thawing mucky clay under subway loading in Shanghai. *Nat Hazards* 72(2):771–787
30. Tang YQ, Yang P, Zhao SK, Zhang X, Wang JX (2008) Characteristics of deformation of saturated soft clay under the load of Shanghai subway line No. 2. *Environ Geol* 54:1197–1203

31. Tang YQ, Zhou J, Hong J, Yang P, Wang JX (2011) Quantitative analysis of the microstructure of Shanghai muddy clay before and after freezing. *Bull Eng Geol Environ* 71(2):309–316
32. Tsytoich NA (1985) *Mechanics of frozen ground*, Translated by Zhan, CQ and Zhu YL. Science Press, Beijing
33. Viklander P (1998) Permeability and volume changes in till due to cyclic freeze–thaw. *Can Geotech J* 35(3):471–477
34. Vyalov SS, Gmshinskii SE (1963) The strength and creep of frozen soils and calculations for ice-soil retaining structures. *US CRREL Transl* 1963:76
35. Wang SF, Yang P, Dai DW, Xue KX, Li DW (2020) A study on micro-pore characteristics of clay due to freeze–thaw and compression by mercury intrusion porosimetry. *Front Earth Sci*. <https://doi.org/10.3389/feart.2019.00344>
36. Wang Z, Wong RCK (2015) Strain-dependent and stress-dependent creep model for a till subject to triaxial compression. *Int J Geomech* 16(3):04015084
37. Wu Z, Deng Y, Cui Y, Zhou A, Feng Q, Xue H (2019) Experimental study on creep behavior in oedometer tests of reconstituted soft clays. *Int J Geomech* 19(3):04018198.1–04018198.10
38. Xu G, Wu W, Qi J (2016) Modeling the viscous behavior of frozen soil with hypoplasticity. *Int J Numer Anal Methods Geom*. <https://doi.org/10.1002/nag.2516>
39. Yang YG, Gao F, Cheng HM, Lai YM, Zhang XX (2014) Researches on the constitutive models of artificial frozen silt in underground engineering. *Adv Mater Sci Eng* 25:1–8
40. Yang YG, Lai YM, Chang XX (2010) Laboratory and theoretical investigations on the deformation and strength behaviors of artificial frozen soil. *Cold Reg Sci Technol* 64:39–45
41. Yao Y, Fang Y (2019) Negative creep of soils. *Can Geotech J*. <https://doi.org/10.1139/cgj-2018-0624>
42. Zhang H, Zhang JM, Zhang Z, My Zhang, Wei Cao (2020) Variation behavior of pore-water pressure in warm frozen soil under load and its relation to deformation. *Acta Geotech* 15(3):603–614
43. Zhao D, Hattab M, Yin ZY, Hicher PY (2018) Dilative behavior of kaolinite under drained creep condition. *Acta Geotech*. <https://doi.org/10.1007/s11440-018-0686-x>
44. Zhou Z, Ma W, Zhang S, Du H, Mu Y, Li G (2016) Multiaxial creep of frozen loess. *Mech Mater* 95(Apr):172–191
45. Zhou ZW, Wei M, Zhang SJ, Mu YH, Li GY (2018) Effect of freeze–thaw cycles in mechanical behaviors of frozen loess. *Cold Reg Sci Tech* 146:9–18
46. Zhu G, Zhu L, Yu C (2017) Rheological properties of soil: a review. *IOP Conf Ser Earth Environ Sci* 64(1):012011

**Publisher's Note** Springer Nature remains neutral with regard to jurisdictional claims in published maps and institutional affiliations.